Das, P. et al. (2020) Band line-up investigation of atomic layer deposited TiAlO and GaAlO on GaN. ECS Journal of Solid State Science and Technology, 9(6), 063003.

There may be differences between this version and the published version. You are advised to consult the publisher's version if you wish to cite from it.

http://eprints.gla.ac.uk/221312/

Deposited on: 24 July 2020

Enlighten – Research publications by members of the University of Glasgow
http://eprints.gla.ac.uk

ECS Journal of Solid State
Science and Technology

The Electrochemical Society
Advancing solid state & electrochemical science & technology

ACCEPTED MANUSCRIPT

Band Line-up Investigation of Atomic Layer Deposited TiAlO and GaAlO on GaN

To cite this article before publication: Partha Das *et al* 2020 *ECS J. Solid State Sci. Technol.* in press https://doi.org/10.1149/2162-8777/aba4f4

Manuscript version: Accepted Manuscript

Accepted Manuscript is "the version of the article accepted for publication including all changes made as a result of the peer review process, and which may also include the addition to the article by IOP Publishing of a header, an article ID, a cover sheet and/or an 'Accepted Manuscript' watermark, but excluding any other editing, typesetting or other changes made by IOP Publishing and/or its licensors"

This Accepted Manuscript is **© 2020 The Author(s). Published by IOP Publishing Ltd.**.

This article can be copied and redistributed on non commercial subject and institutional repositories.

Although reasonable endeavours have been taken to obtain all necessary permissions from third parties to include their copyrighted content within this article, their full citation and copyright line may not be present in this Accepted Manuscript version. Before using any content from this article, please refer to the Version of Record on IOPscience once published for full citation and copyright details, as permissions will likely be required. All third party content is fully copyright protected, unless specifically stated otherwise in the figure caption in the Version of Record.

View the article online for updates and enhancements.

This content was downloaded from IP address 137.111.162.20 on 13/07/2020 at 18:18

Band Line-up Investigation of Atomic Layer Deposited TiAlO and GaAlO on GaN

Journal:	*ECS Journal of Solid State Science and Technology*
Manuscript ID	JSS-100358.R1
Manuscript Type:	Research Paper
Date Submitted by the Author:	08-Jul-2020
Complete List of Authors:	Das, Partha; NIT-Durgapur, ECE Jones, Leanne; University of Liverpool, Department of Electrical Engineering and Electronics; University of Liverpool, Department of Physics and Stephenson Institute for Renewable Energy Gibbon, James; University of Liverpool, Department of Physics and Stephenson Institute for Renewable Energy Dhanak, Vinod; University of Liverpool, Department of Physics and Stephenson Institute for Renewable Energy Manzanera, Teresa; University of Liverpool, School of Engineering Roberts, Joseph ; University of Liverpool, School of Engineering Potter, Richard ; University of Liverpool, School of Engineering Chalker, Paul R; University of Liverpool, School of Engineering Cho, Sung-Jin; University of Glasgow, School of Engineering Thayne, Iain; University of Glasgow, School of Engineering Mahapatra, Rajat; National Institute of Technology Durgapur, Department of Electronics and Communication Engineering Mitrovic, Ivona; University of Liverpool, Electrical Eng and Electronics
Keywords:	GaN, Dielectrics - High-k, Atomic layer deposition, X-ray photoelectron spectroscopy, Band offsets, Kraut method, Metal insulator semiconductor capacitor

SCHOLARONE™
Manuscripts

Accepted Manuscript

1
2
3
4
5
6
7
8
9
10
11
12
13
14
15
16
17
18
19
20
21
22
23
24
25
26
27
28
29
30
31
32
33
34
35
36
37
38
39
40
41
42
43
44
45
46
47
48
49
50
51
52
53
54
55
56
57
58
59
60

Band Line-Up Investigation of Atomic Layer Deposited TiAlO and GaAlO on GaN

Partha Das,[1,z] Leanne A. H. Jones,[2,3] James T. Gibbon,[3]
Vinod R. Dhanak,[3] Teresa Partida-Manzanera,[4] Joseph W. Roberts,[4] Richard Potter,[4] Paul R. Chalker,[4] Sung-Jin Cho,[5] Iain G. Thayne,[5] Rajat Mahapatra,[1,z] and Ivona Z. Mitrovic[2,z]

[1]Department of Electronics and Communication Engineering, National Institute of Technology Durgapur, 713209, India
[2]Department of Electrical Engineering and Electronics, University of Liverpool, L69 3GJ, UK
[3]Department of Physics and Stephenson Institute for Renewable Energy, University of Liverpool, L69 7ZF, UK
[4]School of Engineering, University of Liverpool, L69 3GH, UK
[5]School of Engineering, University of Glasgow, Glasgow G12 8LT, UK

[Z]E-mail: pd.16ec1103@phd.nitdgp.ac.in; ivona@liverpool.ac.uk; rajat.mahapatra@ece.nitdgp.ac.in

A comprehensive study of the band alignments of $Ti_xAl_{1-x}O_y$ (with x = 9%, 16%, 25%, 36%, 100%) and $Ga_xAl_{1-x}O_y$ (x = 5%, 20%, 80% and 95%) fabricated using atomic layer deposition on GaN has been presented using X-ray photoelectron spectroscopy and variable angle spectroscopic ellipsometry. The permittivity, k, has been found to be enhanced from ~10 for 9% Ti in $Ti_xAl_{1-x}O_y$ to 76 for TiO_2, however TiO_2 brings an unfavorable band alignment and a small conduction band offset (< 0.1 eV) with GaN. The latter has been observed for all studied $Ti_xAl_{1-x}O_y$ films deposited on GaN. On the other hand, $Ga_xAl_{1-x}O_y$ films show a substantial increase of the band gap from 4.5 eV for Ga_2O_3 to 5.5 eV for x = 20% Ga and 6.0 eV for x = 5% Ga. A strong suppression of leakage current in associated $Ga_xAl_{1-x}O_y$-based metal insulator semiconductor capacitors has also been observed, showing promise for device applications.

This paper 1043 was accepted to be presented at the Montreal, QC, Meeting of the Society, May 10-14, 2020.

Introduction

GaN high electron mobility transistors (HEMTs) have been commercially available for over 10 years, however gate leakage limits their performance. HEMTs have the advantage of offering simple associated circuit design and fail-safe operation. Currently GaN based metal insulator semiconductor (MIS)-HEMT devices are seen to demonstrate superior performance in power electronics applications over the Schottky gate counterpart, due to its inherently lower gate leakage current, together with the ability to provide a larger

Accepted Manuscript
For Review Only

1 2 3 4 5 6 7 8 9 10 11 12 13 14 15 16 17 18 19 20 21 22 23 24 25 26 27 28 29 30 31 32 33 34 35 36 37 38 39 40 41 42 43 44 45 46 47 48 49 50 51 52 53 54 55 56 57 58 59 60

forward gate voltage swing and an improved gate-drain breakdown voltage [1,2]. High band gap gate dielectric materials, such as Al_2O_3 [3], are preferable as they can provide higher tunneling barriers for electrons and holes resulting in lower gate leakage current. On the other hand, a high dielectric constant (high-k) material is also necessary for improved electrostatic control over the channel and improved on-current, which in-turn results in higher transconductance [4]. The quality of the gate dielectric and the oxide/GaN interface plays a central role in device performance due to potential problems arising from fixed oxide charge, border and interface traps [3]. The leakage current issue has been mitigated using Al_2O_3 [3,5], SiO_2 [6] and Si_3N_4 [7], but comes at a cost of device transconductance degradation and undesirable threshold voltage shifts. A number of high-k dielectrics such as HfO_2 [4,8], ZrO_2 [9,10], Ta_2O_5 [11], $LaLuO_3$ [12] and TiO_2 [13,14] have been investigated. Although the application of these high-k dielectrics has been shown to improve the performance of AlGaN/GaN MIS-HEMTs, several problems remain unsolved, the most serious being the threshold voltage instability [15]. Therefore, further investigation is necessary to advance understanding and improve performance of high-k insulators/GaN interfaces.

In this paper, engineered high-k oxides will be presented; (i) Al_2O_3 alloyed with TiO_2 to boost the oxide permittivity value with the aim of preserving band offsets and (ii) Ga_2O_3 alloyed with Al_2O_3 to increase band gap and maintain good interface quality with GaN. X-ray photoelectron spectroscopy (XPS), inverse photoemission spectroscopy (IPES) and variable angle spectroscopic ellipsometry (VASE) were used to determine the band alignment and interfacial properties of deposited high-k oxide/GaN stacks. TiO_2 is very attractive due to having reported k value of 20-86 [16,17] however, possesses a small band gap of 3.4 eV for amorphous and 3.26 eV for anatase TiO_2 [18] and a low crystallization temperature of 370ºC [19]. Al_2O_3 on the other hand has a sufficient band offset of 1.8-2 eV with AlGaN but suffers from a low dielectric constant of ~7-9 depending on the growth method [20]. The previous studies of Al_2O_3/TiO_2 nanolaminates [21,22] show favorable properties, in particular the optimum between the rather high-k (~30) and low leakage current for 30% Ti [23]. No band offset study has been reported for $Ti_xAl_{1-x}O_y$/GaN. A full band alignment study of $Ti_xAl_{1-x}O_y$/GaN fabricated by atomic layer deposition (ALD) on GaN will be presented for the range of Ti contents (x) of up to 40%.

Furthermore, trivalent Ga_2O_3 is a promising oxide due to its band gap of 4.4 - 4.9 eV [24,25] and a moderate permittivity of 10-14.2 [26]. Thermally oxidized Ga_2O_3 has shown valence band offset (VBO) of 1.4 eV to GaN [27]. A drawback of thermal oxidation is a growth of non-stoichiometric oxide at GaN interface reported to be as $Ga_{(x+2)}N_{3x}O_{(3-3x)}$ [28]. In contrast, ALD has been shown to produce Ga_2O_3 with no interfacial layer with GaN and with low density of interface states of 3.62×10^{11} $cm^{-2}eV^{-1}$ [24]. Despite the good interface with GaN, the issue with using Ga_2O_3 is a small conduction band offset (CBO) of < 1 eV leading to high leakage current. Al_2O_3 has larger band gap (6.4-6.9 eV) and good interface properties to GaN, however Al_2O_3/GaN/AlGaN MIS-HEMTs suffer from threshold voltage instability and current collapse [5,29,30]. The objective of this work was to explore $Ga_xAl_{1-x}O_y$ (x = 5% to 95%) fabricated by ALD with the aim of maintaining sufficiently high band offsets with GaN while preserving good quality interface.

Experimental Details

Accepted Manuscript For Review Only

1 2 3 4 5 6 7 8 9 10 11 12 13 14 15 16 17 18 19 20 21 22 23 24 25 26 27 28 29 30 31 32 33 34 35 36 37 38 39 40 41 42 43 44 45 46 47 48 49 50 51 52 53 54 55 56 57 58 59 60

ALD was performed using a Cambridge Nanotech Savannah 100 reactor for the $Ti_xAl_{1-x}O_y$ films. The TiAlO films of (nominal) 3 nm and 20 nm were deposited using trimethylaluminum (TMA) and titanium isopropoxide (TTIP) as Al and Ti precursors and H_2O as the oxygen-containing co-reactant. The TMA, TTIP and H_2O were transported with 10 sccm zero-grade nitrogen. The TTIP was heated to 90˚C with the substrate held at 200˚C. The number of ALD cycles was used to control the thickness of the films. 1 TMA cycle consisted of a 20 ms TMA dose/2 s purge/20 ms H_2O dose/2 s purge whereas 1 TTIP cycle consisted of a 1 s TTIP dose/10 second purge/20 ms H_2O dose/2 s purge. It is worth mentioning that the film growth rate vs. purge duration showed that for purge times of 2 s and above, the growth rate was constant. For purge times below 2 s, the growth rate increased with decreasing purge duration, indicating the onset of vapour phase reactions. The scanning electron microscope images of deposited Al_2O_3 films (not shown) underpin the growth optimization data and show a uniform, flat plane with no surface particles. Delta doping was utilised to deposit alloyed TiAlO films, where TMA cycles were interspersed periodically within the TTIP cycles. The 2 µm n-GaN/Si substrates were cleaned for 5 minutes in acetone, 5 minutes in isopropyl alcohol and 2 minutes in deionized water (all steps sonicated) followed by drying with N_2. The reference samples of TiAlO films on n-Si(100) were fabricated simultaneously in the ALD chamber to determine thickness and optical properties of the films using VASE. Al top electrodes of different diameters (0.25-2 mm) were deposited on 20 nm TiAlO/GaN by thermal evaporation through a shadow mask to process MIS capacitors for electrical characterization, including capacitance voltage (CV) and current voltage (IV).

In case of Ga_2O_3 and $Ga_xAl_{1-x}O_y$ films, 1 ALD cycle of Ga_2O_3 consisted of the substrate (3 nm GaN/20 nm $Al_{0.2}Ga_{0.8}N$/GaN/accumulation layer/seed layer/Si(111)) being held at 250°C, 0.1 s of triethylgallium, 5 s purge to remove any unreacted precursor or by products, 30 s 20 sscm O_2 flow stabilization, 5 s 300 W O_2 plasma and a final 5 s purge. For the $Ga_xAl_{1-x}O_y$ films, different numbers of Al_2O_3 and Ga_2O_3 ALD cycles were used to vary Al content from 5% to 95%. The Al_2O_3 ALD cycle was a 0.03 s of TMA precursor followed by a 3 s purge, 0.02 s of H_2O and a final 3 s purge. The substrates underwent the same ex-situ chemical cleaning described above. The CV and IV measurements were performed on MIS capacitors, using a ring capacitor layout, with ~200 µm central diameter and a 20 µm gap to the outer ring. The metallization for the outer ring was Ti/Al/Ni/Au (20/120/20/45 nm) followed by rapid thermal anneal (RTA) in N_2 for 30 s at 850°C. The top contact was Ni/Au (20/200 nm). Some MIS devices underwent the forming gas anneal (10% H_2/90% N_2) (FGA) at 430°C for 30 minutes.

Spectroscopic ellipsometry measurements were conducted using a J.A.Woollam VASE ellipsometer with a spectral range of 0.7-5.2 eV at 60-75˚ in 5˚ steps. Preliminary X-ray photoelectron spectroscopy measurements on the $Ga_xAl_{1-x}O_y$ films were performed using a twin anode source. Subsequent measurements of bulk (20 nm) and interfacial (3 nm) oxide/GaN samples were performed in an ultra-high vacuum (UHV) chamber operating at a base pressure of $2x10^{-10}$ mbar. Core level (CL) and valence band (VB) spectra were probed by XPS using a SPECS monochromatic Al Kα X-ray source (hν = 1486.6 eV) operating at 250 W, and a PSP Vacuum Technology electron energy analyzer. The spectrometer was operated with an overall resolution of 0.6 eV measured by the full width at half maximum (FWHM) of Ag $3d_{5/2}$ CL. Charging of the samples was corrected by setting the C 1s peak (arising from adventitious carbon species) to 284.80 eV. The unoccupied density of states in the conduction band (CB) was measured by IPES using a

Accepted Manuscript

Draft only

1 2 3 4 5 6 7 8 9 10 11 12 13 14 15 16 17 18 19 20 21 22 23 24 25 26 27 28 29 30 31 32 33 34 35 36 37 38 39 40 41 42 43 44 45 46 47 48 49 50 51 52 53 54 55 56 57 58 59 60

PSP Vacuum Technology BaO cathode dispenser electron source and an isochromat NaCl photon detector. The IPES detector operates at a nominal resolution of 0.8 eV. The energy scale was calibrated using the Fermi energy of a clean polycrystalline silver foil. A Shirley background was used for the fitting of all XPS CL spectra [31]. The uncertainty of ± 0.05 eV is stated for fitting XPS CLs by Voigt functions.

ALD $Ti_xAl_{1-x}O_y$ films on GaN

Band alignment of $Ti_xAl_{1-x}O_y$ on GaN

Band gap study

The measured and fitted SE (Ψ,Δ) parameters vs. photon energy (E) are shown in Fig. 1. Since Al_2O_3 is a transparent material, Cauchy model [32] was used for the SE data fitting, whereas for TiO_2 a Cody-Lorentz general oscillator model [33] was used due to its UV-absorbing nature. The SE data for TiAlO films were fitted using the Bruggeman Effective Medium Approximation (EMA) model, as the latter allows for a self-consistent choice of the host material. Two materials, Al_2O_3 and TiO_2 as material 1 and material 2 respectively, were placed into the EMA model. The 'EMA % (Mat 2)' parameter was a variable fit parameter representing the percentage of material 2 in the composite. The mean squared error (MSE) between the experimental and theoretical (fitted) (ψ, Δ) versus E curves was in all cases below 5, consistent with a good quality fit of the data shown in Fig. 1. From the ellipsometry modeling, the Ti content in the films (x) was found to be 9% (2:1=Al:Ti cycles), 16% (1:1 = Al:Ti cycles), 25% (1:2 = Al:Ti cycles) and 36% (1:4 = Al:Ti cycles) in agreement with values calculated from the ALD growth rates and number of cycles used for Al_2O_3 and TiO_2 to fabricate mixed oxide films (Fig. 2). It has been observed that the growth rate decreases for films with increasing Ti percentage.

The thickness of the films (summarized in Table I), refractive index (n) and extinction coefficient (κ) were extracted from the SE modelling; the absorption coefficient (α) can be found from the extinction coefficient as

$$\alpha = \frac{4\pi\kappa(E)E}{hc} \quad (1)$$

where h is the Planck's constant, c is the speed of light, and E is the photon energy. The plots of α vs. E for $Ti_xAl_{1-x}O_y$ and TiO_2 are shown in Fig. 3(a). The linear extrapolation of the leading absorption edges seen in Fig. 3(a) gives the band gap (E_g) values (± 0.1 eV) for TiO_2 of 3.65 eV and for $Ti_xAl_{1-x}O_y$ films varying from 4.28 eV to 3.88 eV as Ti content is increased from 9% to 36% respectively. The latter are in agreement with band gap data of 4.0 eV for 20% Ti and 3.8 eV for 30-40% Ti extracted from reflection electron energy loss spectroscopy (REELS) [23]. In the most recent study of ALD $Ti_xAl_{1-x}O_y$ films, the band gap of 4.3 eV and 4.1 eV has been inferred for films with 33% Ti and 40% Ti respectively, from UV-vis absorption spectra plotted as $(\alpha h\nu)^2$ vs. E [34]. The reported values for the optical band gap of TiO_2 have been found to be dependent on the crystallinity of the film and found to be 3.2 eV [23], 3.66-3.73 eV [34], 3.37 eV [35] to 3.7 eV [36]. The band gap of Al_2O_3 was extracted from the O 1s energy loss feature from the XPS measurement [37] shown in Fig. 3(b) and was found to be 6.48 ± 0. 25 eV, in close agreement with optical band gap value (6.43 eV) extracted by vacuum ultra-violet (VUV)-VASE using α-method [38] and theoretical value (6.36 eV) obtained by density functional supercell calculations [39].

Accepted Manuscript
For Review Only

Accepted Manuscript
For Review Only

Band offsets study

The Al 2p, Ti 2p and O 1s XPS CLs measured for $Ti_xAl_{1-x}O_y$/GaN stacks are shown in Figs. 4(a), (b) and (c) respectively. It can be seen that the Al 2p CL shifts to the lower binding energy (BE) for up to 0.63 eV (Fig. 4(a)) while the Ti $2p_{3/2}$ BE increases by 0.13 eV (Fig. 4(b)) with the increase of Ti % in the $Ti_xAl_{1-x}O_y$ films. A similar trend has been reported when TiO_2 and Al_2O_3 are mixed [21,22] and is explained by the differing electronegativities of Al (1.61) and Ti (1.54), creating different tendencies for Al and Ti to attract and donate electrons respectively. This suggests that an alloy is formed and not laminates. The O 1s CLs also indicate the formation of alloyed layers, as shown in Fig. 4(c). The O 1s CL shifts as a function of Al:Ti ratio between the two BE extremities of Al_2O_3 (531.16 eV) and TiO_2 (530.0 eV). Furthermore, the FWHM of O 1s CL decreases from binary Al_2O_3 to TiO_2, which again suggests an alloy being formed rather than separate layers of both (laminate), as the FWHM would be larger if the peak contained components from Al_2O_3 and TiO_2 simultaneously [23].

Figures 5(a)-(b) depict the fitting of Al 2p and O 1s CLs for bulk Al_2O_3, while Figs. 5(c)-(d) refer to fitted Ti 2p and O 1s for bulk TiO_2. As seen in Fig. 5(a), the Al 2p is symmetric, suggesting only one environment of Al. The BE of the Al 2p was found at 74.54 eV, in agreement with the reported values [40,41] when different C 1s spectra calibration has been considered. The O 1s peak shown in Fig. 5(b) is fitted with two components, at 531.16 eV associated with Al-O bonds [40] and the other at 531.89 eV likely to be related to O-H species. The latter is not thought to be related to Al-OH bonds since both Al 2p and Al 2s (not shown) CLs are found to be symmetric, indicating only one environment of Al [42,43]. The VB spectrum for Al_2O_3 bulk sample is shown in the inset of Fig. 5(a) with valence band maximum (VBM) at 3.65 eV, which gives the Al 2p CL BE to VBM difference of δ_{Al2O3} = 70.89 eV. The Ti 2p CL shown in Fig. 5(c) is fitted with two components (Ti $2p_{3/2}$ and Ti $2p_{1/2}$), which indicates the presence of only one oxidation state of Ti (+4). The FWHM of the Ti $2p_{1/2}$ is larger than that of the Ti $2p_{3/2}$ due to the Coster-Kronig process [44]. Therefore, the area and the BE position of the Ti $2p_{1/2}$ were constrained and the FWHM was set as a fitting parameter. The O 1s CL had a secondary contribution at the similar BE as the one in Al_2O_3 (Fig. 5(d)), which was attributed to O-H bonds. The latter were not thought to be Ti-OH bonds as the Ti CLs only consisted of Ti-O contribution. It is likely that this peak is associated with carbon contamination, possibly to CO-OH species on the surface. The VBM of bulk TiO_2 was at 2.83 eV (see inset in Fig. 5(c)) and the Ti $2p_{3/2}$ to VBM difference was found to be δ_{TiO2} = 455.70 eV. The valence band offset between oxide and GaN can be calculated from XPS and the Kraut method [45] using the equation:

$$VBO = \delta_{SUB} - \delta_{OXIDE} + \delta_{INT} \quad (2)$$

where δ_{SUB} refers to the binding energy difference of respective CL in the substrate (in our case, the Ga $2p_{3/2}$ CL) and VBM for GaN substrate, δ_{OXIDE} of chosen CL in the bulk of the oxide (Al 2p or Ti $2p_{3/2}$) and VBM for bulk oxide sample, and δ_{INT} of Ga $2p_{3/2}$ and Al 2p (or Ti $2p_{3/2}$) from respective oxide and GaN for interfacial oxide/GaN sample. Fig. 6 shows fitted CL spectra and VBM referring to TiAlO oxide with 25% Ti and the three terms in Eq. (2) are calculated to be δ_{SUB} = 1115.24 eV (Fig. 6(a)), δ_{INT} = 1043.60 eV (Fig. 6(b)) and δ_{TiAlO} = 71.0 eV (Fig. 6(c)). Note that the Ti 2p peaks sit in the middle of the Ga

1 2 3 4 5 6 7 8 9 10 11 12 13 14 15 16 17 18 19 20 21 22 23 24 25 26 27 28 29 30 31 32 33 34 35 36 37 38 39 40 41 42 43 44 45 46 47 48 49 50 51 52 53 54 55 56 57 58 59 60

Augers, hence the Al 2p CL was used in the Kraut method for all $Ti_xAl_{1-x}O_y$/GaN samples. In case of TiO_2/GaN, the Ti $2p_{3/2}$ was used, but VBO (Eq. (2)) was also cross-checked with Ti 3p CL.

A summary of CL positions, thicknesses, band gaps and band offsets for all $Ti_xAl_{1-x}O_y$/GaN samples is given in Table I. The conduction band offset is calculated from

$$CBO = E_g^{OXIDE} - E_g^{GaN} - VBO \quad (3)$$

where E_g^{OXIDE}, E_g^{GaN} refer to band gaps of oxide (see Table I) and GaN (=3.4 eV [46]) respectively. It is worth mentioning that there is no significant shift of Ga $2p_{3/2}$ for interfacial TiAlO/GaN samples when compared to the BE value of 1117.67 eV for GaN substrate, being indicative of a negligible band bending (BB) at the interface (see Table I). In case of TiO_2/GaN, the Ga $2p_{3/2}$ shifts slightly towards higher BEs, and this could be a signature of a small downward BB of 0.22 eV. Furthermore, the XPS CL fitting results suggest no interfacial layer is formed between the TiAlO and GaN. The latter is underpinned by (i) the BE positions and FWHM of the O 1s CLs remaining the same (no other oxygen environment), (ii) the Ga 2p FWHM being constant (indicating no new Ga environment) and (iii) symmetric nature of the Ga 2p and Al 2p CLs, again indicating no new environments for all interfacial mixed oxide samples. Only for interfacial TiO_2/GaN sample, there was an additional component in the Ti 2p CL fitting at 557.33 eV (not shown), which was attributed to Ti_2O_3 in line with the previous XPS studies [47]. This interfacial layer and a possible existence of Ga-O bonds at the interface could be a source of positive charges on the GaN surface [48], which is leading to accumulated surface and resulting in a small downward band bending for this sample.

The VBO for Al_2O_3 of 1.13 ± 0.25 eV is in excellent agreement with the recent theoretical (1.17 eV) [39] and experimental (1.07 eV) studies (see Ref. 48 and references therein). As can be seen from Table I, the VBO decreases from 0.84 eV for 9% Ti to 0.61 eV for 36% Ti mixed oxide. By inserting optical band gap values from Fig. 3(a) in Eq. (3), the CBO is found to be very small <0.05 eV for mixed oxides with up to 25% Ti. In case of 36% Ti sample and TiO_2/GaN, type I heterojunction is observed with CBO of around -0.1 eV. TiO_2 was found to have VBO of 0.39 ± 0.25 eV. In the previous XPS study of TiO_2/GaN, Ga 3d and Ti 3p CLs were used in the Kraut method where the VBO of 0.09 ± 0.25 eV was found [13]; both Ga 3d and Ti 3p are shallow CLs and could hybridise with valence orbitals which in turn distorts the line shape of the core level, reducing the accuracy of the binding energy values and hence the VBO value. Therefore, in this work we have used Ga $2p_{3/2}$ and Ti $2p_{3/2}$ CLs. Furthermore, the δ_{SUB} for GaN has been measured to be 17.05 eV [13], being much smaller than widely cited literature values of 17.7-17.8 eV [48]; if the latter value for δ_{SUB} is used in the Kraut method, the VBO is 0.55 ± 0.25 eV [13] and is in line with the measured value in this work within the accuracy of the method. It has also been reported recently that VBO for TiO_2/AlGaN is 0.56 eV and for Al_2O_3/AlGaN is 1.00 eV by XPS and the Kraut method [14]; from these values, the VBO of 1.56 eV for TiO_2/Al_2O_3 interface can be deduced in excellent agreement with 1.52 eV from this study calculated from measured VBOs for TiO_2/GaN (0.39 eV) and Al_2O_3/GaN (1.13 eV) (see Table I). It is worth mentioning that due to a smaller band gap of 3.0 eV for TiO_2 used for the band alignment in Ref. 13, a type I TiO_2/GaN heterojunction has been deduced. In this study, the measured optical band gap by VASE has been found to be larger (3.65 eV, Fig. 3(a), Table I) and a type II TiO_2/GaN heterointerface is inferred. The measured TiO_2 band

Accepted Manuscript
For Review Only

1
2
3
4
5
6
7
8
9
10
11
12
13
14
15
16
17
18
19
20
21
22
23
24
25
26
27
28
29
30
31
32
33
34
35
36
37
38
39
40
41
42
43
44
45
46
47
48
49
50
51
52
53
54
55
56
57
58
59
60

gap in this work correlates with more recent studies, where values of ~3.7 eV [34,36] and 3.5 eV [49] have been stated. Note that the difference in valence band maxima for the bulk oxide samples and GaN are in close agreement with the VBOs calculated using the Kraut method and Eq. (2), providing further evidence of negligible band bending at oxide/GaN interfaces for samples listed in Table I. Furthermore, a gradual decrease of VBO with increasing Ti % can be seen from Table I, while CBO stays mainly constant for $Ti_xAl_{1-x}O_y$/GaN samples. Similar has been observed for $Ti_xAl_{1-x}O_y$ ALD films on Si [34] and on GaAs [49], where a gradual increase in VBO with decreasing Ti content is evident, while CBO values stay close to that of TiO_2 being nearly constant and independent of x.

Electrical properties of $Ti_xAl_{1-x}O_y$ films on GaN

CV and IV measurements of MIS capacitors based on $Ti_xAl_{1-x}O_y$ alloy films, with the compositional range of 9–36% Ti, were carried out for the thickness range from 24 nm to 31 nm (Table I). The current density (J) vs. gate voltage plots are shown in Fig. 7(a), clearly indicating a rise of gate leakage when Ti% is increased in the mixed oxide films. Fig. 7(b) shows J at 1 MV/cm of the $Ti_xAl_{1-x}O_y$ with compositional range in this work and Ref. 23. The Ti-rich film (36% Ti) has J = 2.98×10^{-1} A/cm^2 decreasing to 3.95×10^{-5} A/cm^2 for Al-rich film (9% Ti), being comparable to the previously reported values of RTA annealed (700ºC for 60 seconds in N_2) ALD deposited $Ti_xAl_{1-x}O_y$ films [23]. The permittivity of the oxide films was extracted from the CV plots at 1 MHz; the results are depicted in Fig. 7(b) and show increase of k from 7.0 (Al_2O_3), 10.2 (9% Ti), 15.6 (16% Ti), 24.4 (25% Ti), 32.9 (36% Ti) to 75.8 (TiO_2) with increasing Ti content in the mixed oxides. The k values obtained for Al_2O_3 and TiO_2 are in line with the range reported in the literature [16,20].

ALD $Ga_xAl_{1-x}O_y$ films on GaN

Band alignment of Ga_2O_3 on GaN

Figure 8(a) depicts the Ga $2p_{3/2}$ XPS CL spectra for the bulk GaN (top), interfacial Ga_2O_3/GaN (middle) and bulk Ga_2O_3 (bottom) samples. The Kraut method [45] and Eq. (2) was used to find the VBO between Ga_2O_3 and GaN. It can be seen for the interfacial Ga_2O_3/GaN sample that the Ga $2p_{3/2}$ peak is resolved into two components, at the low BE side at (i) 1117.74 eV related to Ga-N bond, and (ii) at high BE side at 1118.26 eV referring to Ga-O bond. This is due to the electronegativity of oxygen being greater than that of nitrogen leading to the Ga CL from Ga_2O_3 to be found at higher BE. Hence, the respective δ_{INT} = 0.52 eV. For the GaN substrate and bulk Ga_2O_3 (of 22.2 nm thickness as measured by VASE), the position of the Ga $2p_{3/2}$ peak was found at 1117.22 eV (Fig. 8(a), top) and 1118.30 eV (Fig. 8(a), bottom), respectively. The valence band maximum was found by extrapolating the valence band edge and finding the point of intersection between this linear fit and the background linear fit (Fig. 8(b)). For GaN and Ga_2O_3 the VBMs (± 0.25 eV) were found to be 2.07 eV and 3.36 eV, respectively. These values were used to calculate δ_{SUB}= 1115.15 eV and δ_{Ga2O3}= 1114.94 eV. The VBO for Ga_2O_3/GaN is then calculated from Eq. (2) and found to be 0.73 ± 0.25 eV. An IPES spectra were used to find the conduction band minima (CBM, ± 0.25 eV) for GaN (1.60 eV) and Ga_2O_3 (1.23 eV) as shown in the left-hand side of Fig. 8(b). Since both the VBM and CBM are measured with respect to the Fermi level, the addition of the two values gives the band gap of the material.

Accepted Manuscript
For Review Only

1 2 3 4 5 6 7 8 9 10 11 12 13 14 15 16 17 18 19 20 21 22 23 24 25 26 27 28 29 30 31 32 33 34 35 36 37 38 39 40 41 42 43 44 45 46 47 48 49 50 51 52 53 54 55 56 57 58 59 60

Therefore, the band gap (± 0.25 eV) measured by XPS/IPES is found to be 3.67 eV for GaN and 4.59 eV for Ga_2O_3.

There is an indication of substantial downward band bending of 0.52 eV from the shift of Ga $2p_{3/2}$ in GaN substrate and in Ga_2O_3/GaN (see dashed lines and an arrow in Fig. 8(a)). The angle resolved (AR)-XPS data confirms a ~0.5 eV shift of Ga $2p_{3/2}$ peak towards the higher BEs with decrease of take-off angle (TOA) from normal to the surface (90°, BE = 1117.78 eV) to 15° from the surface (BE = 1118.28 eV), providing further evidence of substantial downward band bending at Ga_2O_3/GaN interface. The downward BB of GaN surface has been reported following similar ex-situ chemical cleaning as in this work [50]. The observation of an accumulated GaN surface has been explained by a significant positive charge density residing within the native oxide [50]. A possible source for the positive charge may be (i) interfacial fixed charge with energy states between the CBM of the native oxide and GaN [50]; or (ii) a possible polarity inversion of the GaN surface, that is a change in the spontaneous polarization charge from negative to positive due to the formation of Ga–O bonds.

The band gap of GaN from Fig. 8(b) (top) is higher (3.67 eV) than the reported optical band gap of 3.4 eV [46], but it is within the experimental error (± 0.25 eV) of the IPES measurements. The optical band gap of Ga_2O_3 extracted from the VASE B-spline model and associated absorption coefficient vs. photon energy curve shown in Fig. 9(a) is 4.47 ± 0.1 eV and compares to 4.59 ± 0.25 eV derived from the XPS/IPES (Fig. 8(b), bottom). The obtained values are in agreement with the literature [24,25].

Using the VBM values for Ga_2O_3 and GaN, the VBO for Ga_2O_3/GaN is estimated to be 1.29 eV, a larger value than the one measured from the Kraut method (0.73 eV). However, by taking into account the observed downward BB of 0.52 eV, the VBO further from the interface can be deduced to be 1.25 ± 0.25 eV close to the estimated value of 1.29 eV. The latter is in agreement with the VBO of 1.4 ± 0.08 eV reported for β−Ga_2O_3/GaN heterostructure derived by the Kraut method where no BB has been observed at the interface [27]. The resultant CBO is calculated using Eq. (3) taking into account the optical band gap for Ga_2O_3 and gives a value of 0.34 ± 0.25 eV.

Band alignment of $Ga_xAl_{1-x}O_y$ on GaN

A set of 20 nm (nominal) $Ga_xAl_{1-x}O_y$ on GaN samples were fabricated varying the Ga:Al ALD cycles from 1:19, 1:4, 4:1 and 19:1, referring to x of 5% Ga, 20% Ga, 80% Ga and 95% Ga respectively. The band gaps of the samples were found using the energy loss feature of the O 1s XPS spectra; Fig. 9(b) refers to spectra with high Al content showing a significant increase in the band gap from 5.50 eV (80% Al) to 5.98 eV (95% Al).

The valence band maxima extracted from the linear extrapolation of the VB edge (Fig. 9(c)) give values of 3.29 eV for 5% Al and 3.6 ± 0.2 eV for 20% Al $Ga_xAl_{1-x}O_y$ film. For increased Al content (above 20%) in the $Ga_xAl_{1-x}O_y$ films (1:19 and 1:4 Ga:Al cycles), the VBM remains constant at ~ 3.6 eV. This suggests that there is no change in VBO when Al content is increased, i.e. VBO can be estimated to be ~1.5 eV and thus the band gap rise results in the CBO increasing.

Electrical properties of $Ga_xAl_{1-x}O_y$ on GaN

Accepted Manuscript
For Review Only

1
2
3
4
5
6
7
8
9
10
11
12
13
14
15
16
17
18
19
20
21
22
23
24
25
26
27
28
29
30
31
32
33
34
35
36
37
38
39
40
41
42
43
44
45
46
47
48
49
50
51
52
53
54
55
56
57
58
59
60

MIS capacitor devices exhibited very high leakage current for samples with high Ga content and no measurable CV plots; therefore, the focus was on investigating only films with high Al content. The CBO calculated for Ga_2O_3 gave a small value of 0.34 ± 0.25 eV which explains the very high leakage currents observed for MIS capacitors based on Ga_2O_3 and low Al content $Ga_xAl_{1-x}O_y$ films (see Fig. 9(d) for 4:1 and 19:1 Ga:Al cycles). For high Al content (80% and 95%), the band gap increases significantly (Fig. 9(b)) and since the VBO is observed not to change, the CBO is found to increase to 0.6 eV (for 80% Al) and to 1.1 eV (for 95% Al). Fig. 9(d) shows significant reduction of leakage current of several orders of magnitude for samples with high Al content (1:19 and 1:4 Ga:Al cycles) in agreement with the band line-up study. The permittivity of $Ga_xAl_{1-x}O_y$ films is found to be ~ 7 from CV plots close to the value of k for Al_2O_3 film (Fig. 7(b)) as these films have high Al content.

In summary, the band alignments of $Ti_xAl_{1-x}O_y$/GaN and $Ga_xAl_{1-x}O_y$/GaN stacks studied in this work are presented schematically in Fig. 10.

Conclusion

In this paper, $Ti_xAl_{1-x}O_y$ (x = 9% to 100%) and $Ga_xAl_{1-x}O_y$ (x= 5%, 20%, 80% and 95%) films have been fabricated using atomic layer deposition with the aim of achieving favorable band alignment with GaN for MIS-HEMT applications. X-ray photoelectron spectroscopy, inverse photoemission spectroscopy and variable angle spectroscopic ellipsometry were used to estimate the band alignment and interfacial properties. Although the permittivity of $Ti_xAl_{1-x}O_y$ increases significantly from 7 for Al_2O_3 to 24.4 for 25% Ti and 32.9 for 36% Ti, the band line-up of these mixed oxides is not ideal as conduction band offsets with GaN were found to be ≤ 0.1 eV. The VBO is found to decrease from 0.8 eV for 9% Ti to 0.6 eV for 36% Ti mixed oxide film. The TiO_2/GaN was found to be type II heterojunction interface with VBO = 0.39 ± 0.25 eV. The results from Ga_2O_3 and $Ga_xAl_{1-x}O_y$ films point to substantial increase of the band gap from ~4.6 eV for Ga_2O_3 to 5.9 eV for the 1:19 Ga:Al ALD cycles (5% Ga) GaAlO sample and a strong suppression of leakage current. The VBO for Ga_2O_3/GaN interface is found to be 0.73 ± 0.25 eV with a substantial downward band bending observed at the GaN surface. The valence band offset for $Ga_xAl_{1-x}O_y$ with x=5% and 20% remains constant, indicating an increase in CBO in line with improved gate leakage current. The results are promising for future applications in GaN based devices.

Acknowledgments

The authors acknowledge UGC-UKIERI project numbers IND/CONT/G/17-18/18 and F.No.184-1/2018(IC) “Dielectric engineering on GaN for sustainable energy applications” funded by the British Council; UKRI GCRF GIAA award 2018/19 and “Digital in India” project no. EP/P510981/1 funded by the EPSRC, UK.

References

1. H. Amano, Y. Baines, E. Beam, M. Borga, T. Bouchet, P. R. Chalker, M. Charles, K. J. Chen, N. Chowdhury, R. Chu, C. D. Santi, M. M.D. Souza, S. Decoutere, L.

Accepted Manuscript
For Review Only

D. Cioccio, B. Eckardt, T. Egawa , P. Fay , J. J. Freedsman, L. Guido, O. Häberlen, G. Haynes, T. Heckel, D. Hemakumara, P. Houston, J. Hu, M. Hua, Q. Huang, A. Huang, S. Jiang, H. Kawai, D. Kinzer, M. Kuball, A. Kumar, K. B. Lee, X. Li, D. Marcon, M. März, R. McCarthy, G. Meneghesso, M. Meneghini, E. Morvan, A. Nakajima, E. M. S. Narayanan, S. Oliver, T. Palacios, D. Piedra, M. Plissonnier, R. Reddy, M. Sun, I. Thayne, A. Torres, N. Trivellin, V. Unni, M. J. Uren, M. V. Hove, D. J. Wallis, J. Wang, J. Xie, S. Yagi, S. Yang, C. Youtsey, R. Yu, E. Zanoni, S. Zeltner, and Y. Zhang, *J. Phys. D. Appl. Phys.*, **51**, 163001 (2018).

2. K. J. Chen, O. Häberlen, A. Lidow, C. L. Tsai, T. Ueda, Y. Uemoto, and Y. Wu, *IEEE Trans. Electron Devices*, **64**, 779 (2017).
3. T. Hashizume, S. Ootomo, and H. Hasegawa, *Appl. Phys. Lett*., **83**, 2952 (2003).
4. C. Liu, E. F. Chor, and L. S. Tan, *Appl. Phys. Lett.*, **88**, 173504 (2006).
5. D. Ye, B. Yang, K. K. Ng, J. Bude, G. D. Wilk, S. Halder, and J. C. M. Hwang, *Appl. Phys. Lett*., **86**, 063501 (2005).
6. P. Kordoš, G. Heidelberger, J. Bernát, A. Fox, M. Marso, and H. Lüth, *Appl. Phys. Lett.*, **87**, 143501 (2005).
7. S. Arulkumaran, T. Egawa, H. Ishikawa, T. Jimbo, and Y. Sano, *Appl. Phys. Lett*., **84**, 613 (2004).
8. F. Tian and E. F. Chor, *J. Electrochem. Soc*., **157**, H557 (2010).
9. H. Jiang, C. Liu, K. W. Ng, C.W. Tang, and K. M. Lau, *IEEE Trans. Electron Devices*, **65**, 5337 (2018).
10. T. J. Anderson, V. D. Wheeler, D. I. Shahin, M. J. Tadjer, A. D. Koehler, K. D. Hobart, A. Christou, F. J. Kub, and C. R. Eddy, *Appl. Phys. Express*, **9**, 071003 (2016).
11. D. A. Deen, D. F. Storm, R. Bass, D. J. Meyer, D. S. Katzer, S. C. Binari, J. W. Lacis, and T. Gougousi, *Appl. Phys. Lett*., **98**, 023506 (2011).
12. S. Yang, S. Huang, M. Schnee, Q. T. Zhao, J. Schubert, and K. J. Chen, *IEEE Trans. Electron Devices*, **60**, 3040 (2013).
13. P. J. Hansen, V. Vaithyanathan, Y. Wu, T. Mates, S. Heikman, U. K. Mishra, R. A. York, D. G. Schlom, and J. S. Specka, *J. Vac. Sci. Technol. B*, **23**, 499 (2005).
14. A. Rawat, M. Meer, V. K. Surana, N. Bhardwaj, V. Pendem, N. S. Garigapati, Y. Yadav, S. Ganguly, and D. Saha, *IEEE Trans. Electron Devices*, **65**, 3725 (2018).
15. Z. Yatabe, J.T. Asubar, and T. Hashizume, J. Phys. D: Appl. Phys., **49**, 393001 (2016).
16. T. Fuyuki and H. Matsunami, *Jpn. J. Appl. Phys*., **25**, 1288 (1986).
17. J. Yan, D. C. Gilmer, S. A. Campbell, W. L. Gladfelter, and P. G. Schmid, *J. Vac. Sci. Technol. B*, **14**, 1706 (1996).
18. J. Aarik, A. Aidla, A.-A. Kiisler, T. Uustare, and V. Sammelselg, *Thin Solid Films*, **305**, 270 (1997).
19. Q. Xie, J. Musschoot, D. Deduytsche, R. L. V. Meirhaeghe, C. Detavernier, S. V. D. Berghe, Y. L. Jiang, G. P. Ru, B. Z. Li, and X. P. Qu, *J. Electrochem. Soc*., **155**, H688 (2008).
20. X. Qin, L. Cheng, S. McDonnell, A. Azcatl, H. Zhu, J. Kim, and R. M. Wallace, *J. Mater. Sci: Mat. in El.*, **26**, 4638 (2015).
21. B. M. Reddy, B. Chowdhury, and P. G. Smirniotis, *Appl. Cat. A: General*, **211**, 19 (2001).
22. L. H. Kim, K. Kim, S. Park, Y. J. Jeong, H. Kim, D. S. Chung, S. H. Kim, and C. E. Park, *ACS Appl. Mat. & Inter*., **6**, 6731 (2014).

Accepted Manuscript

For Review Only

1 2 3 4 5 6 7 8 9 10 11 12 13 14 15 16 17 18 19 20 21 22 23 24 25 26 27 28 29 30 31 32 33 34 35 36 37 38 39 40 41 42 43 44 45 46 47 48 49 50 51 52 53 54 55 56 57 58 59 60

23. A. P. Alekhin, A. A. Chouprik, S. A. Gudkova, A. M. Markeev, Y. Y. Lebedinskii, Y. A. Matveyev, and A. V. Zenkevich, *J. Vac. Sci. Techn. B*, **29**, 01A302 (2011).
24. H-Y. Shih, F-C. Chu, A. Das, C-Y. Lee, M-J. Chen, and R-M. Lin, *Nanoscale Research Letters*, **11**, 235 (2016).
25. D-W. Choi, W-B. Chung, and J-S. Park, *Thin Solid Films*, **546**, 31 (2013).
26. H. S. Oon and K. Y. Cheong, *Mat. Sci. Semicond. Proc.*, **16**, 1217 (2013).
27. W. Wei , Z. Qin, S. Fan, Z. Li, K. Shi, Q. Zhu, and G. Zhang, *Nanoscale Research Letters*, **7**, 562 (2012).
28. S. D. Wolter, J. M. DeLucca, S. E. Mohney, R. S. Kern, and C. P. Kuo, *Thin Solid Films*, **371**, 153 (2000).
29. P. Lagger, C. Ostermaier, G. Pobegen, and D. Pogany, Proc. IEEE IEDM, p. 299 (2012).
30. S. Huang, S. Yang, J. Roberts, and K. J. Chen, *Jpn. J. Appl. Phys.*, **50**, 110202 (2011).
31. D. A. Shirley, *Phys. Rev. B*, **5**, 4709 (1972).
32. Z. Wang, R. Zhang, H. Lu, X. Chen, Y. Sun, Y. Zhang, Y. Wei, J. Xu, S. Wang, Y. Zheng, and L. Chen, *Nanoscale Res. Lett.*, **10**:46, 1 (2015).
33. M. Horprathum, P. Chindaudom, P. Limnonthakul, P. Eiamchai, N. Nuntawong, V. Patthanasettakul, A. Pokaipisit, and P. Limsuwan, *J. Appl. Phys.*, **108**, 013522 (2010).
34. J. Gao, G. He, L. Hao, D. Wang and L. Zhao, *RSC Adv.*, **10,** 14733 (2020).
35. N. Y. Garces, D. J. Meyer, V. D. Wheeler, Z. Liliental-Weber, D. K. Gaskill, and C. R. Eddy Jr., *J. Vac. Sci. Techn. B,* **32**, 03D101 (2014).
36. Y. Shi, R. Zhang, H. Zheng, D. Li, W. Wei, X. Chen, Y. Sun, Y. Wei, H. Lu, N. Dai, and L. Chen, *Nanoscale Res. Lett.*, **12**, 1 (2017).
37. M. T. Nichols, W. Li, D. Pei, G. A. Antonelli, Q. Lin, S. Banna, Y. Nishi, and J. L. Shohet, *J. Appl. Phys.*, **115**, 094105 (2014).
38. I. Z. Mitrovic, M. Althobaiti, A. D. Weerakkody, V. R. Dhanak, N. Sedghi, S. Hall, P. R. Chalker, D. Tsoutsou, and A. Dimoulas, *J. Appl. Phys.*, **115**, 114102 (2014).
39. Z. Zhang, Y. Guo, and J. Robertson*, Appl. Phys. Lett.*, **114**, 161601 (2019).
40. T. Gougousi, D. Barua, E. D. Young, and G. N. Parsons, *Chem. Mater.*, **17**, 5093 (2005).
41. B. Lee, S. Park, H. Kim, K. Cho, E. M. Vogel, M. J. Kim, R. M. Wallace, and J. Kim, *Appl. Phys. Lett.*, **92**, 203102 (2008).
42. I. Iatsunskyi, M. Kempinski, M. Jancelewicz, K. Zaleski, S. Jurga, and V. Smyntyna, *Vacuum*, **113**, 52 (2015).
43. J. Haeberle, K. Henkel, H. Gargouri, F. Naumann, B. Gruska, M. Arens, M. Tallarida, and D. Schmeißer, *J. Nanotechnol.*, **4**, 732 (2013).
44. D. Coster and R. D. L. Kronig, *Physica,* **48**, 13 (1928).
45. E. A. Kraut, R. W. Grant, J. R. Waldrop, and S. P. Eowalczyk, *Phys. Rev. Lett.*, **44**, 1620 (1980).
46. J. Wagner, H. Obloh, M. Kunzer, M. Maier, K. Köhler, and B. Johs, *J. Appl. Phys.*, **89**, 2779 (2001).
47. M. J. Jackman, A. G. Thomas, and C. Muryn, *J. Phys. Chem. C*, **119**, 13682 (2015).
48. S. N. Supardan, P. Das, J. D. Major, A. Hannah, Z. H. Zaidi, R. Mahapatra, K. B. Lee, R. Valizadeh, P. A. Houston, S. Hall, V. R. Dhanak, and I. Z. Mitrovic, *J. Phys. D: Appl. Phys.*, **53**, 075303 (2020).
49. Y. An, C. Mahata, C. Lee, S. Choi, Y-C. Byun, Y-S. Kang, T. Lee, J. Kim, M-H. Choand, and H. Kim, *J. Phys. D: Appl. Phys.,* **48**, 415302 (2015).

Accepted Manuscript
For Review Only

1
2
3
4
5
6
7
8
9
10
11
12
13
14
15
16
17
18
19
20
21
22
23
24
25
26
27
28
29
30
31
32
33
34
35
36
37
38
39
40
41
42
43
44
45
46
47
48
49
50
51
52
53
54
55
56
57
58
59
60

50. T. L. Duan, J. S. Pan, and D. S. Ang, *ECS J. Solid State Sci. Technol.*, **5**, P514 (2016).

Accepted Manuscript
For Review Only

1
2
3
4
5
6
7
8
9
10
11
12
13
14
15
16
17
18
19
20
21
22
23
24
25
26
27
28
29
30
31
32
33
34
35
36
37
38
39
40
41
42
43
44
45
46
47
48
49
50
51
52
53
54
55
56
57
58
59
60

Tables

TABLE I. A summary of fitted binding energies of Al 2p, Ti $2p_{3/2}$, Ga $2p_{3/2}$ XPS CLs and extrapolated VBM for bulk and interfacial $Ti_xAl_{1-x}O_y$/GaN samples fabricated by ALD in this work. The thickness and optical band gap are determined using VASE. The VBO (± 0.25 eV) of deposited oxides on GaN stated is calculated from the Kraut method (Eq. (2)), while CBO using Eq. (3). Al_2O_3 and TiO_2 are added as reference samples.

Sample	Thickness (nm)	Al 2p (eV)	Ti $2p_{3/2}$ (eV)	Ga $2p_{3/2}$ (eV)	VBM (eV)	E_g (eV)	VBO (eV)	CBO (eV)
GaN		--	--	1117.67	2.43	3.4*	--	--
Al_2O_3	19.1	74.54	--	--	3.65	6.48**	1.13	1.95
	3.0	74.50		1117.72	--			
9% Ti	23.8	74.02	458.66	--	3.13	4.28	0.84	0.04
	3.7	74.23	458.86	1117.74	--			
16% Ti	26.6	74.01	458.64	--	2.97	4.20	0.76	0.04
	3.9	74.14	458.73	1117.58	--			
25% Ti	30.9	74.08	458.74	--	3.08	4.02	0.64	0.02
	3.9	74.12	458.75	1117.72	--			
36% Ti	28.1	73.91	458.66	--	3.01	3.88	0.61	-0.13
	4.0	74.07	458.75	1117.80	--			
TiO_2	17.0	--	458.53	--	2.83	3.65	0.39	-0.14
	3.4		458.74	1117.89	--			

*Ref. 46; **XPS

Accepted Manuscript
For Review Only

1
2
3
4
5
6
7
8
9
10
11
12
13
14
15
16
17
18
19
20
21
22
23
24
25
26
27
28
29
30
31
32
33
34
35
36
37
38
39
40
41
42
43
44
45
46
47
48
49
50
51
52
53
54
55
56
57
58
59
60

Figures

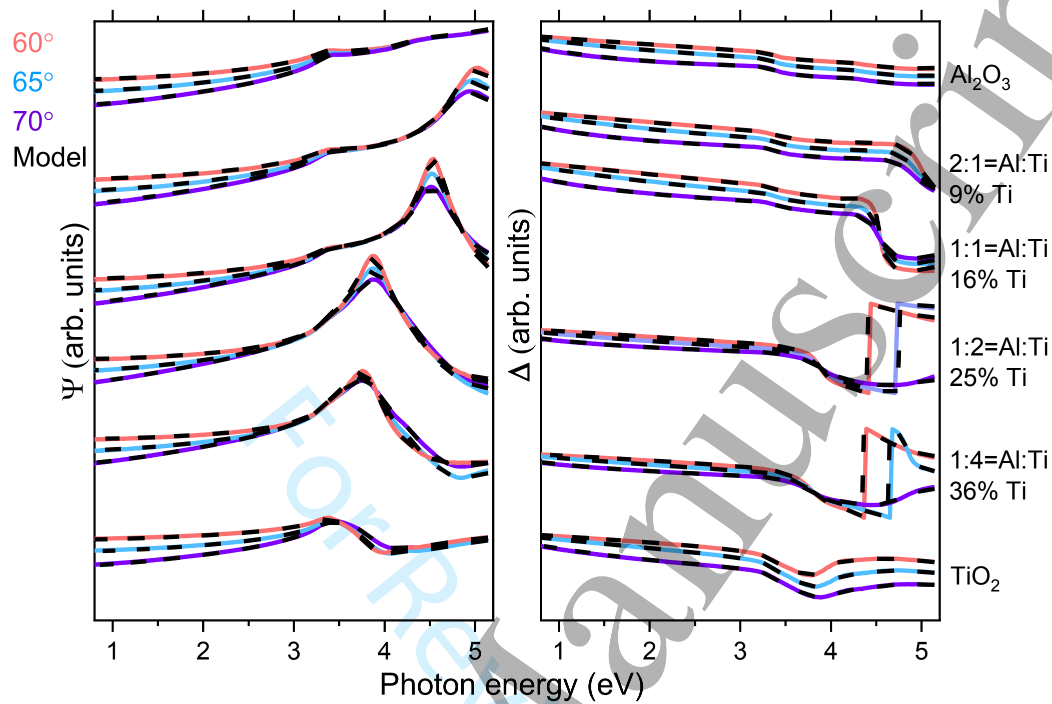

Figure 1. Measured and fitted spectroscopic ellipsometric (Ψ,Δ) parameters vs. photon energy for ALD $Ti_xAl_{1-x}O_y$ (x < 40%) films with Al_2O_3 and TiO_2 as reference samples.

Accepted Manuscript
For Review Only

1
2
3
4
5
6
7
8
9
10
11
12
13
14
15
16
17
18
19
20
21
22
23
24
25
26
27
28
29
30
31
32
33
34
35
36
37
38
39
40
41
42
43
44
45
46
47
48
49
50
51
52
53
54
55
56
57
58
59
60

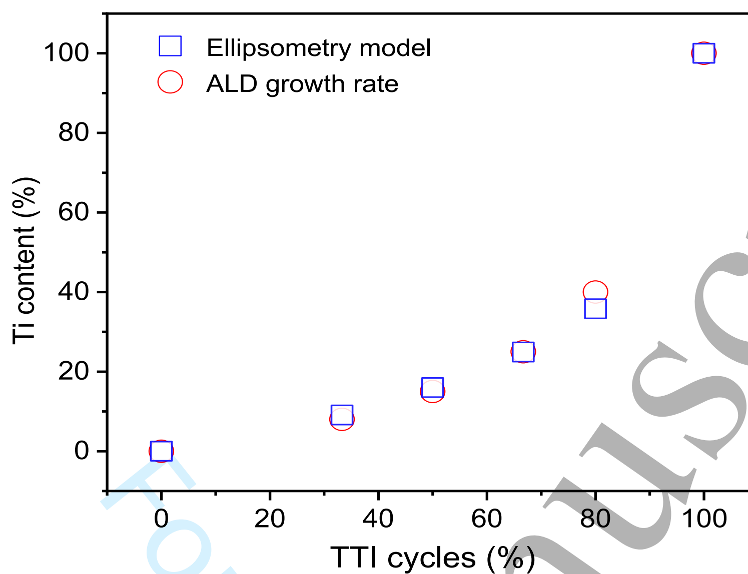

Figure 2. The derived Ti content (x) for the ALD mixed oxide films ($Ti_xAl_{1-x}O_y$) from ellipsometry data and theoretically predicted from the ALD growth rate.

Accepted Manuscript

For Review Only

1
2
3
4
5
6
7
8
9
10
11
12
13
14
15
16
17
18
19
20
21
22
23
24
25
26
27
28
29
30
31
32
33
34
35
36
37
38
39
40
41
42
43
44
45
46
47
48
49
50
51
52
53
54
55
56
57
58
59
60

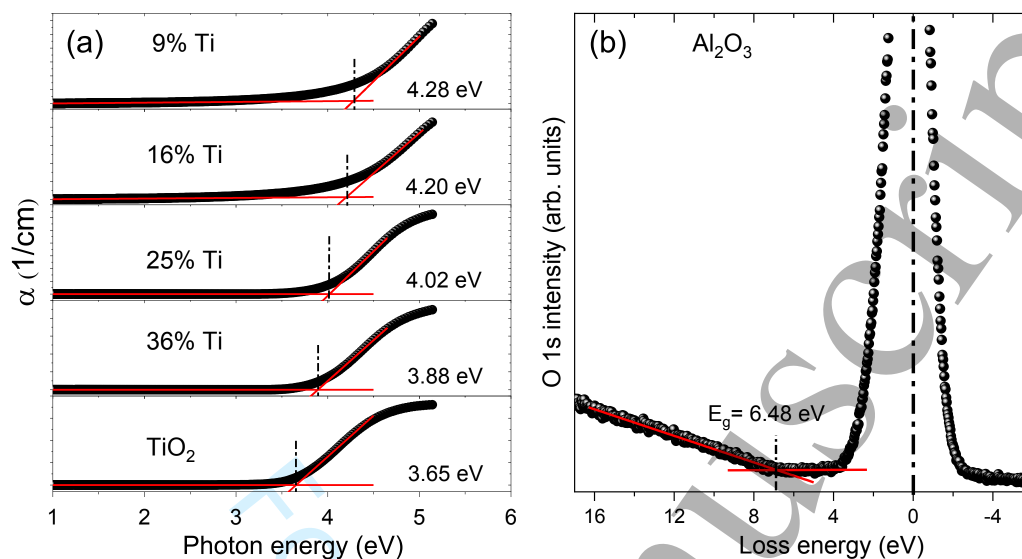

Figure 3. (a) α vs. photon energy plots for $Ti_xAl_{1-x}O_y$ films, with x varying from 9% to 100% (TiO_2); (b) XPS O 1s energy loss spectrum depicting extraction of the band gap for Al_2O_3.

Accepted Manuscript

For Review Only

1
2
3
4
5
6
7
8
9
10
11
12
13
14
15
16
17
18
19
20
21
22
23
24
25
26
27
28
29
30
31
32
33
34
35
36
37
38
39
40
41
42
43
44
45
46
47
48
49
50
51
52
53
54
55
56
57
58
59
60

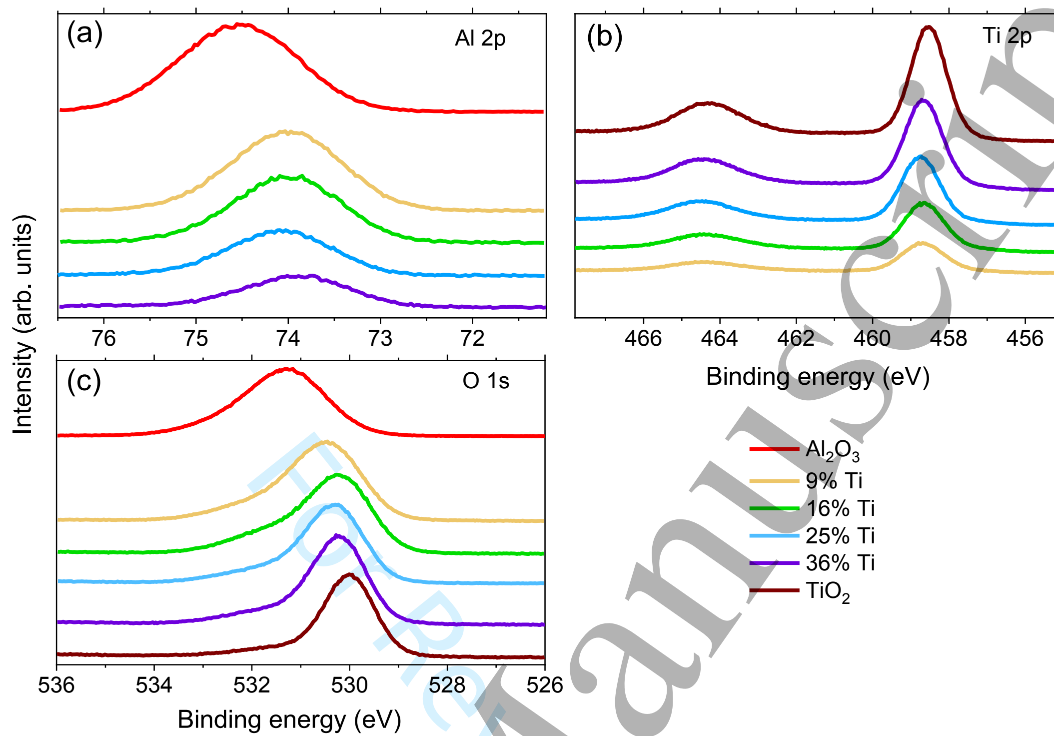

Figure 4. (a) Al 2p, (b) Ti 2p and (c) O 1s XPS CL spectra for bulk (20 nm) ALD TiAlO/GaN stacks with Al_2O_3/GaN and TiO_2/GaN as reference samples.

Accepted Manuscript
For Review Only

1
2
3
4
5
6
7
8
9
10
11
12
13
14
15
16
17
18
19
20
21
22
23
24
25
26
27
28
29
30
31
32
33
34
35
36
37
38
39
40
41
42
43
44
45
46
47
48
49
50
51
52
53
54
55
56
57
58
59
60

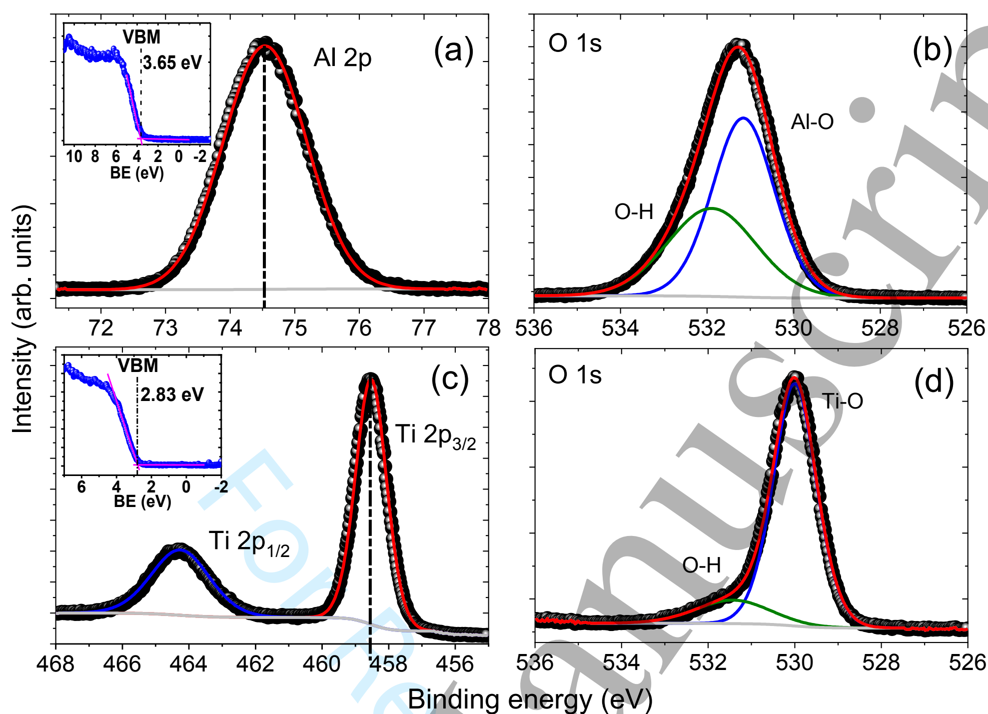

Figure 5. (a)-(b) Al 2p and O 1s fitted CL spectra for bulk Al_2O_3 film; (c)-(d) Ti 2p and O 1s fitted CL spectra for bulk TiO_2 film. The insets in (a) and (c) refer to valence band spectra depicting extraction of valence band maxima for Al_2O_3 and TiO_2 respectively.

Accepted Manuscript
For Review Only

1
2
3
4
5
6
7
8
9
10
11
12
13
14
15
16
17
18
19
20
21
22
23
24
25
26
27
28
29
30
31
32
33
34
35
36
37
38
39
40
41
42
43
44
45
46
47
48
49
50
51
52
53
54
55
56
57
58
59
60

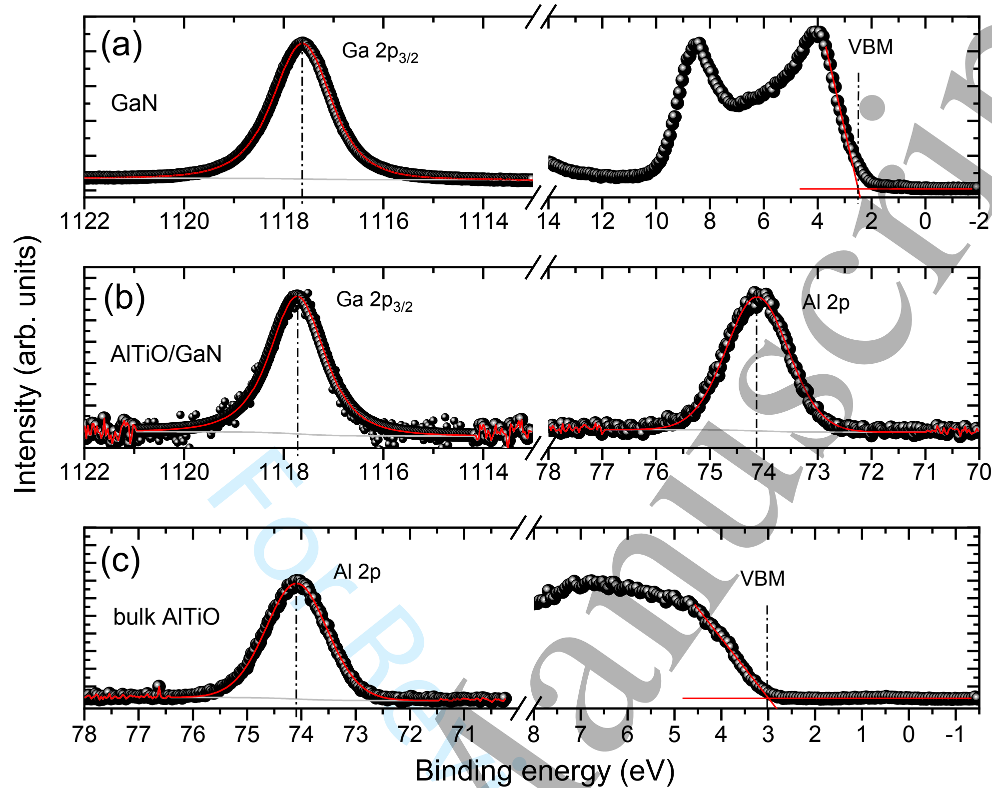

Figure 6. Ga $2p_{3/2}$, Al 2p XPS CLs and VBM extraction from (a) GaN substrate; (b) interfacial 3.9 nm $Ti_xAl_{1-x}O_y$/GaN and (c) bulk 30.9 nm $Ti_xAl_{1-x}O_y$, for x= 25%.

Accepted Manuscript
For Review Only

1
2
3
4
5
6
7
8
9
10
11
12
13
14
15
16
17
18
19
20
21
22
23
24
25
26
27
28
29
30
31
32
33
34
35
36
37
38
39
40
41
42
43
44
45
46
47
48
49
50
51
52
53
54
55
56
57
58
59
60

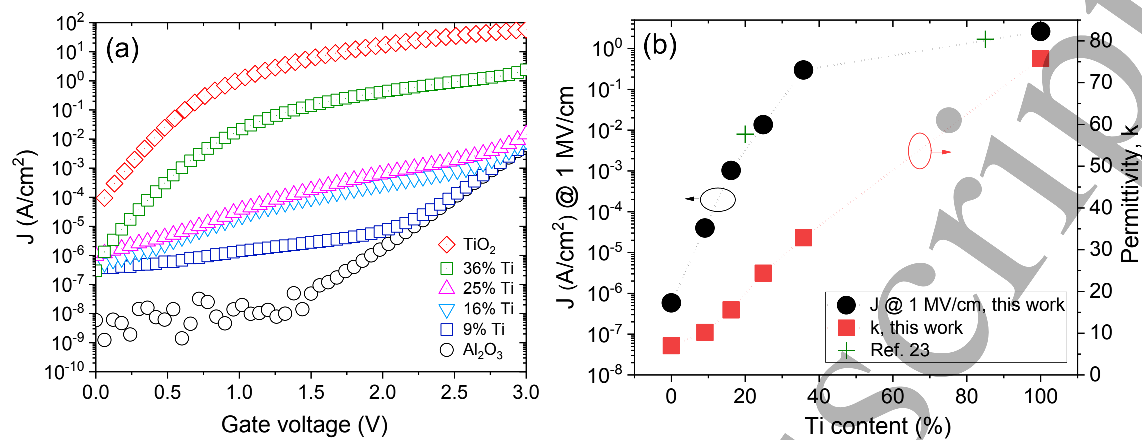

Figure 7. (a) Current density (J) vs. gate voltage; (b) J at 1 MV/cm and k vs % Ti measured from MIS capacitors based on ALD $Ti_xAl_{1-x}O_y$ films. (Device area A = 4.9x10^{-8} m^2.)

Accepted Manuscript
For Review Only

1
2
3
4
5
6
7
8
9
10
11
12
13
14
15
16
17
18
19
20
21
22
23
24
25
26
27
28
29
30
31
32
33
34
35
36
37
38
39
40
41
42
43
44
45
46
47
48
49
50
51
52
53
54
55
56
57
58
59
60

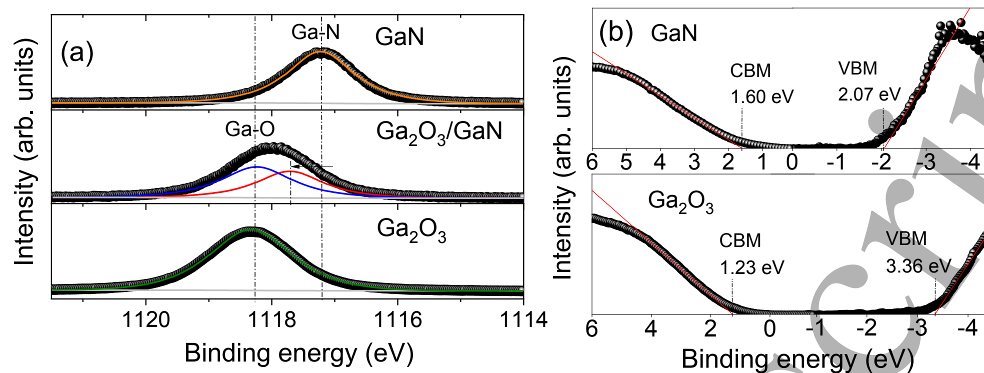

Figure 8. (a) Ga $2p_{3/2}$ XPS CL fitting for GaN (top), interfacial Ga_2O_3/GaN (middle) and bulk Ga_2O_3 (bottom) ALD film; (b) IPES spectra for GaN (top) and Ga_2O_3 (bottom).

Accepted Manuscript
For Review Only

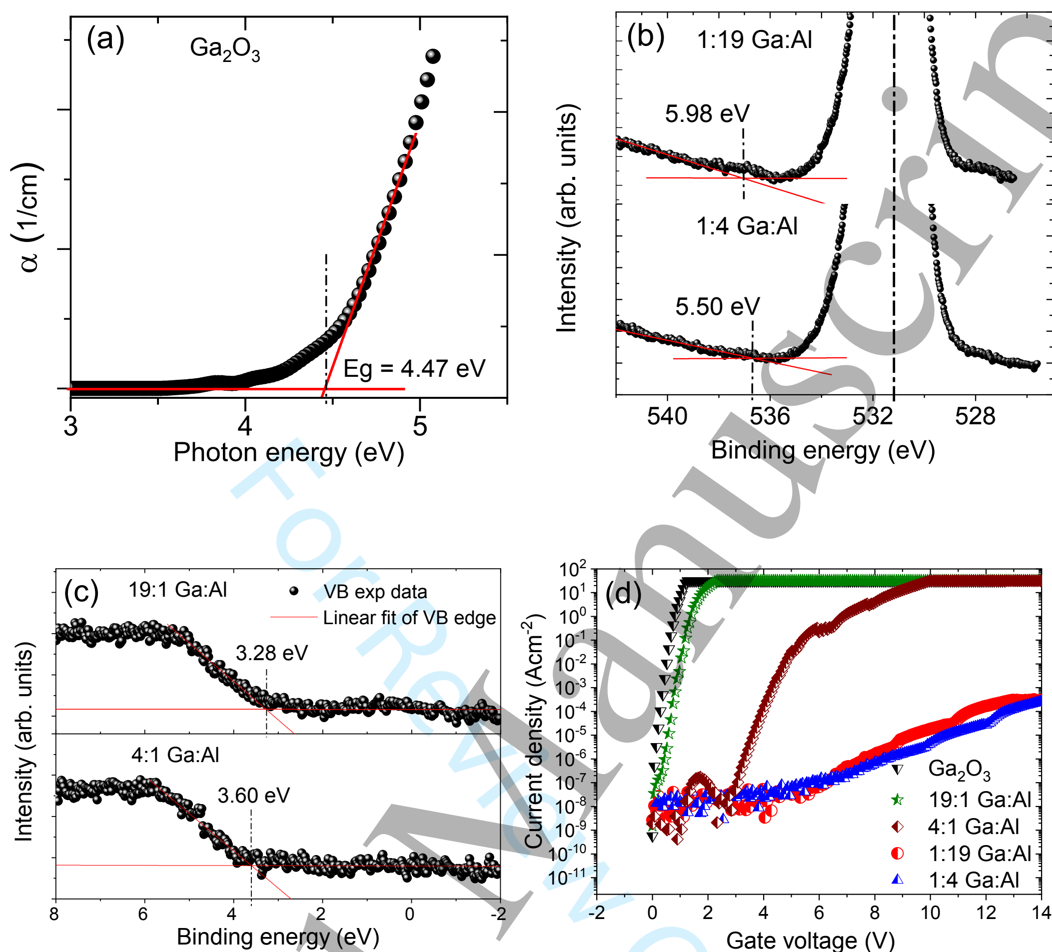

Figure 9. α vs. E for Ga_2O_3; (b) XPS O 1s energy loss spectra for 5% Ga (95% Al, 1:19 = Ga:Al) and 20% Ga (80% Al, 1:4 = Ga:Al); (c) VB spectra of $Ga_xAl_{1-x}O_y$ for x = 5% and 20%, depicting extraction of VBM; (d) Current density vs. voltage for associated MIS capacitors.

Accepted Manuscript
For Review Only

1
2
3
4
5
6
7
8
9
10
11
12
13
14
15
16
17
18
19
20
21
22
23
24
25
26
27
28
29
30
31
32
33
34
35
36
37
38
39
40
41
42
43
44
45
46
47
48
49
50
51
52
53
54
55
56
57
58
59
60

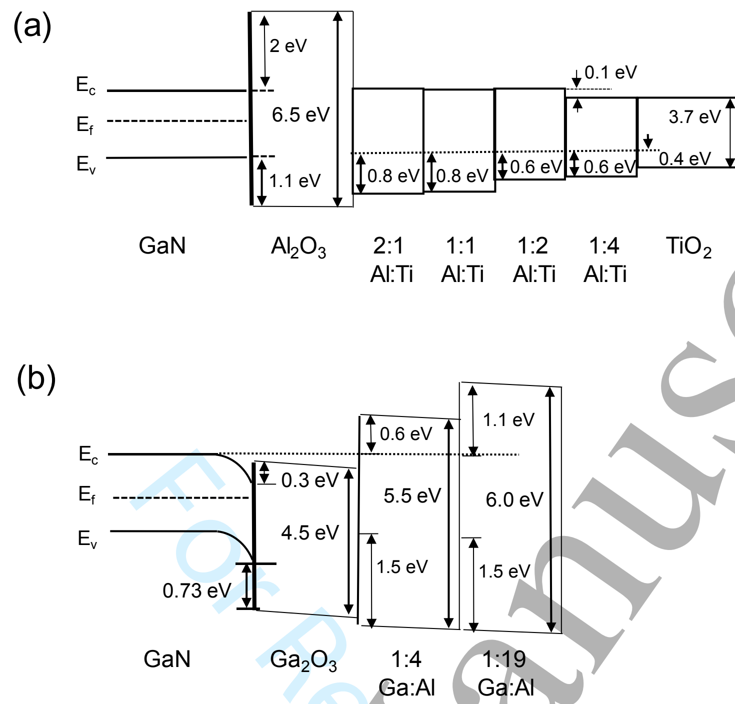

Figure 10. The experimentally derived band line-up for ALD processed (a) $Ti_xAl_{1-x}O_y$/GaN and (b) $Ga_xAl_{1-x}O_y$/GaN stacks. (The diagrams are not to scale.)

Accepted Manuscript
For Review Only